2013-12-09

Temperature dependence of diffusion length, lifetime and minority electron mobility in GaInP

Schultes, F.J.; Haegel, N.M.; Christian, T.; Alberi, K.; Fluegel, B.; Jones-Albertus, R.; Pickett, E.; Liu, T.; Misra, P.; Sukiasyan,A....

Journal Name: Applied Physics Letters; Journal Volume: 103; Journal Issue: 24; Other Information: (c) 2013 AIP Publishing LLC; Country of input: International Atomic Energy Agency (IAEA)
http://hdl.handle.net/10945/57270

Temperature dependence of diffusion length, lifetime and minority electron mobility in GaInP

F. J. Schultes,[1] T. Christian,[2] R. Jones-Albertus,[3] E. Pickett,[3] K. Alberi,[2] B. Fluegel,[2] T. Liu,[3] P. Misra,[3] A. Sukiasyan,[3] H. Yuen,[3] and N. M. Haegel[1,a)]
[1]*Physics Department, Naval Postgraduate School, Monterey, California 93943, USA*
[2]*National Renewable Energy Laboratory, Golden, Colorado 80401, USA*
[3]*Solar Junction, Inc., San Jose, California 95131, USA*

(Received 31 October 2013; accepted 22 November 2013; published online 12 December 2013)

The mobility of electrons in double heterostructures of p-type $Ga_{0.50}In_{0.50}P$ has been determined by measuring minority carrier diffusion length and lifetime. The minority electron mobility increases monotonically from 300 K to 5 K, limited primarily by optical phonon and alloy scattering. Comparison to majority electron mobility over the same temperature range in comparably doped samples shows a significant reduction in ionized impurity scattering at lower temperatures, due to differences in interaction of repulsive versus attractive carriers with ionized dopant sites. These results should be useful in modeling and optimization for multi-junction solar cells and other optoelectronic devices. © *2013 AIP Publishing LLC*. [http://dx.doi.org/10.1063/1.4847635]

Minority carrier transport plays a critical role in the performance of devices, such as solar cells, light emitting diodes, semiconductor lasers, and bipolar transistors. While minority carrier lifetime can vary greatly, depending on doping and defect density, minority carrier mobility is a more fundamental material property. It is important for device modeling and optimization and also provides insight into the physics of carrier scattering. Direct experimental measurements that lead to minority carrier mobilities, however, are quite limited. This is especially true for the ternary alloys used in the highest efficiency multi-junction solar cells. Multiple devices have now reached efficiencies in excess of 43% over the past 5 years and single cell efficiencies are predicted to exceed 50% with future work.[1,2]

The temperature and doping dependence of minority carrier mobility can be very different than that of majority carrier mobility. Majority carrier mobilities are routinely measured using the Hall effect. For minority carriers, particularly in doped materials, electron-beam-induced current (EBIC) or Haynes-Shockley type measurements can be performed to determine the minority carrier diffusion length L_d. When coupled to independent measurements of lifetime (τ), generally through time-resolved photoluminescence (TRPL), the minority carrier mobility μ can be obtained, since $L_d = \sqrt{\frac{kT}{e}\mu\tau}$. However, both EBIC and traditional Haynes-Shockley measurements require electrical contact and are often not well suited to the heterostructures of interest. As a result, minority carrier mobility data for ternary semiconductors are extremely limited.

In this paper, we report temperature-dependent measurements of the minority carrier mobility in $Ga_{0.5}In_{0.5}P$. This ternary material is lattice-matched to GaAs and used as the largest bandgap top cell material in all the multi-junction solar cells that have held recent records for highest single device efficiency.[1] We utilize transport imaging, which is a contact-free optical approach to the measurement of minority carrier diffusion length, over the temperature range from 300 K to 5 K, combined with TRPL measurements over the same temperature range on the same samples.

The samples are double heterostructures of GaInP, with $Al_{0.25}Ga_{0.25}In_{0.5}P$ barrier layers. The heterostructures were grown by molecular beam epitaxy on GaAs substrates, with a GaAs MBE-grown buffer layer. The GaInP layers of interest were 500 nm thick, with top and bottom barrier layers of 50 and 200 nm, respectively. Cathodoluminescence spectroscopy measurements indicated that the only significant luminescence was from the GaInP layers, with a peak emission at ~650–660 nm at room temperature depending on doping. Samples studied were either intentionally p-type doped with Be or nominally undoped.

Minority carrier diffusion lengths were measured via transport imaging in a scanning electron microscope,[3,4] which involves measuring the spatial variation of the luminescence produced when excess carriers are generated in a fixed location by an electron beam. The concept is illustrated in Figure 1. The samples are placed in a scanning electron microscope, where the electron beam passes through a small hole in the optical microscope reflecting surface. For the uniform films of interest here, the electron beam is scanned repeatedly over a line of length ~80 μm. The resulting luminescence is collected with an optical microscope and detected by a CCD camera. Figure 1(a) shows a schematic of the system.

Figure 1(b) illustrates the basic concept: carriers created at a point will diffuse and some fraction will recombine along the way, over a characteristic distance given by the minority carrier diffusion length. By maintaining the spatial information in the recombination luminescence, the minority carrier diffusion length can be obtained directly from the optical image. In this regard, transport imaging is different than scanning cathodoluminescence or photoluminescence, where spatial information about the sample is obtained by scanning the excitation point and assuming that all luminescence is associated with the point of generation. Transport imaging

a)Author to whom correspondence should be addressed. Electronic mail: nmhaegel@nps.edu

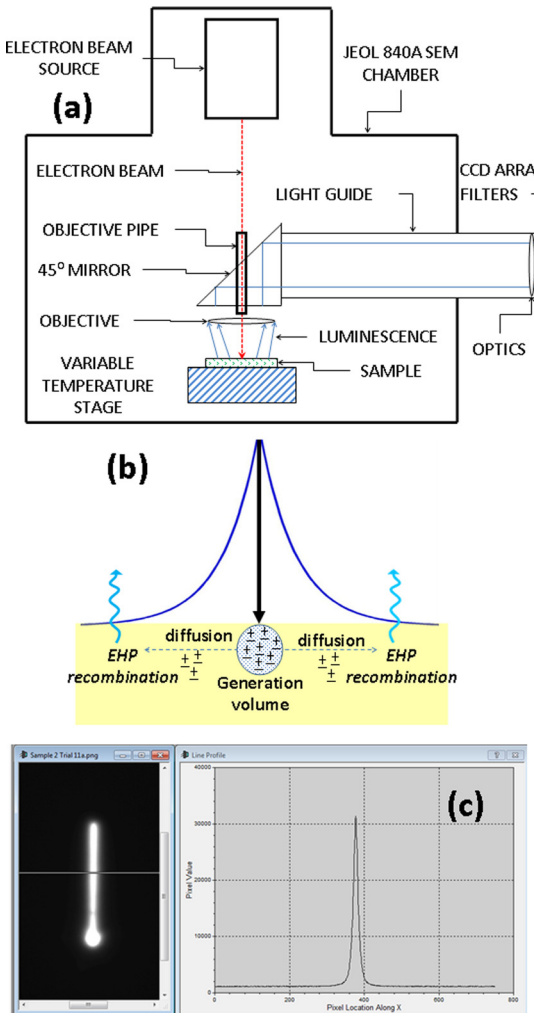

FIG. 1. Transport imaging in the SEM. (a) Excitation and optical collection system. (b) Carrier generation, diffusion, and recombination. (c) SEM line scan and resulting optical image and luminescence distribution.

takes advantage of the fact that this assumption is not actually valid—the luminescence has a distribution pattern around the point of generation.

Figure 1(c) shows an example of an optical image that is obtained and the distribution of the luminescence perpendicular to the path of the electron beam. The symmetry that results from line excitation on a thin film means that the diffusion lengths can be extracted from analysis of the distribution $I = I_O e^{(-x/L_d)}$, where I is the intensity, x is the distance from the excitation line, and L_d is the minority carrier diffusion length. This approximation is good when the length of the excitation line is long and the thickness of the film is small compared to the diffusion length of interest. The modeling for the diffusion profiles for transport imaging in a thin film with low surface recombination for both spot mode and line mode excitation has been published previously.[3–5]

All transport imaging measurements presented in this paper were performed with an electron beam energy of 5 keV and a probe current of 6×10^{-11} A. Low energy electrons and low probe current minimize the generation volume and injection level, respectively. In the low injection limit, the lifetime can be treated as a constant. We estimate the steady state carrier change in majority hole population at this level of excitation to be $\sim 6 \times 10^{14}\,\mathrm{cm}^{-3}$, supporting the low injection approximation for both the intentionally doped and the nominally undoped materials. Variable temperature measurements were achieved using a liquid helium flow system that cools the cold stage within the SEM chamber. The temperature is monitored with a temperature-sensing diode embedded in the cold stage.

TRPL was performed using a pulsed, tunable titanium-sapphire laser with pulse lengths of ~150 fs. The laser output was frequency doubled to produce excitation pulses with a wavelength of 405 nm and a total deposited energy per pulse of $\sim 5\,\mu\mathrm{J/cm}^2$ under standard excitation conditions. Sample luminescence was collected using a streak camera and integrated across the full width of the luminescence spectrum, approximately 40 nm, to produce TRPL decay curves. Decay times did not vary significantly with spectral energy for the excitation power densities considered here. Samples were mounted in a closed-cycle helium cryostat for variable temperature measurements between 5 and 300 K.

Diffusion length and TRPL measurements as a function of temperature were performed on both doped and nominally undoped samples. Doping for the p-type sample was $1 \times 10^{17}\,\mathrm{cm}^{-3}$. The nominally undoped material is also p-type, with doping in the range of 10^{15}–$10^{16}\,\mathrm{cm}^{-3}$. Doping levels are monitored by periodic Hall effect measurements on samples grown with comparable flux levels of the dopant material.

Figure 2 shows the results for the diffusion length measurements as a function of temperature comparing the doped and nominally undoped material. Figure 3 shows the variable temperature minority carrier lifetime measurements. Both transport imaging and TRPL measurements were performed on the same samples. The diffusion length measurements indicate a difference with the doping, with a longer diffusion length in the nominally undoped material of about a factor of two. The diffusion lengths are not strongly temperature dependent in either case. The lifetime measurements also indicate variation with doping and a decreasing lifetime with decreasing temperature.

Combining the diffusion length and lifetime measurements, the minority carrier mobility (electrons in p-type material) can be obtained. This is shown as a function of temperature in Figure 4. Lifetimes were interpolated for cases where more data points were available from the

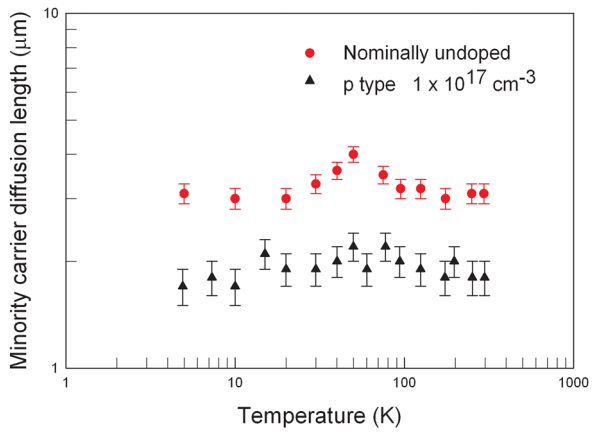

FIG. 2. Minority carrier (electron) diffusion length as a function of temperature for doped and nominally undoped p-type GaInP.

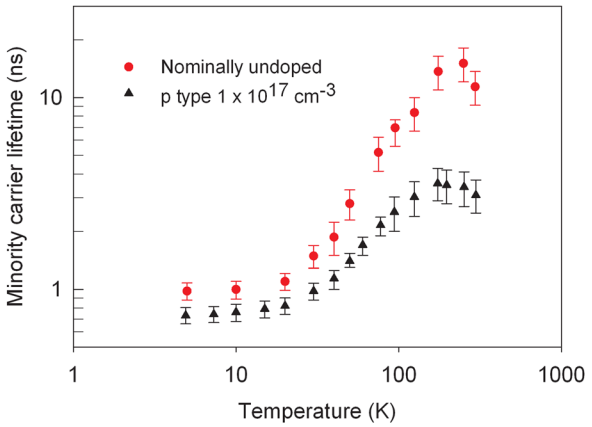

FIG. 3. Minority carrier (electron) lifetime as a function of temperature for doped and nominally undoped p-type GaInP.

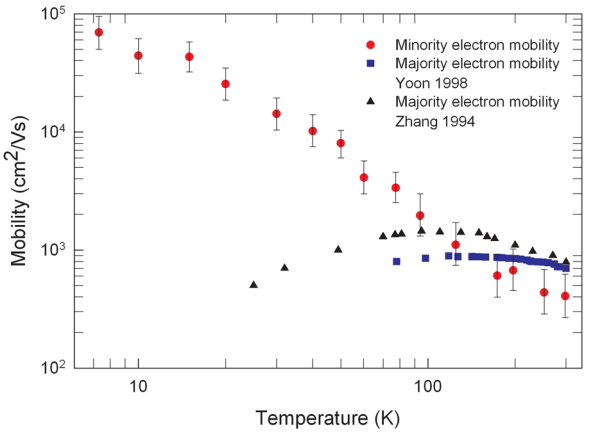

FIG. 5. Minority electron mobility in p-type GaInP as a function of temperature (this work) compared to majority electron mobility in comparably doped n-type GaInP (Refs 10 and 11).

transport imaging measurements. Within the error bars, the mobility values are quite similar at room temperature for the two materials. This is consistent with theoretical calculations of minority electron mobility as a function of doping in the ternary alloy AlGaAs,[6] which showed that the dependence of mobility on doping decreases significantly with increasing degree of alloying, i.e., increasing mole fraction y in $Ga_{1-y}Al_yAs$. In this case, the 50/50 alloying and the relatively low doping levels make the lattice scattering dominant at room temperature.

The overall temperature dependence is similar for both materials. The results suggest polar optical scattering[7] as the dominant scattering mechanism at higher temperatures with alloy scattering[8] playing a role at lower temperatures. Combined modeling of these scattering mechanisms for majority carriers in GaInP has been presented in Refs. 9 and 10 for comparison to Hall effect measurements. However, no corresponding comparisons to theory exist for minority carriers.

We find monotonically increasing values for the minority electron mobility with decreasing temperature. This is in contrast to the decrease in mobility that is generally observed for majority carrier scattering in doped materials. In Figure 5, we compare our minority carrier electron mobility values to the temperature dependent ***majority*** electron mobility data available in the literature from Hall effect

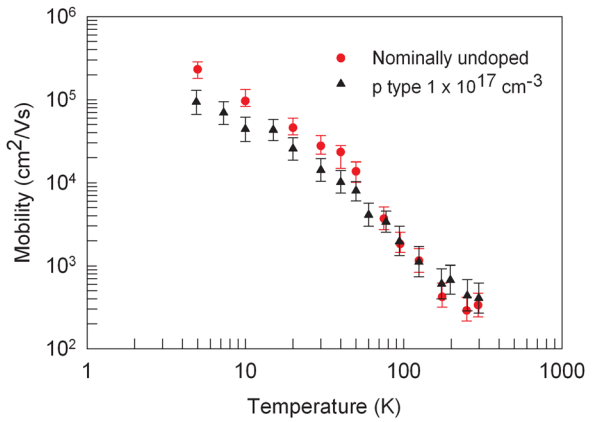

FIG. 4. Minority carrier (electron) mobility as a function of temperature for doped and nominally undoped p-type GaInP.

measurements on comparably doped n-type GaInP. Data presented in Figure 5 are for net electron concentrations of $6.5 \times 10^{16}\,cm^{-3}$ (Ref. 11) and $7.8 \times 10^{16}\,cm^{-3}$ (Ref. 10). One sees that the majority carrier mobility shows a much weaker temperature dependence and decreases with decreasing temperature in the lower temperature regime.

Measurements to enable similar variable temperature comparison between majority and minority electron mobility have been presented for more heavily doped Si and GaAs, with minority carrier mobilities measured via bipolar transistor measurements[12] and lateral photocurrent collection[13] in Si and via cut-off frequencies in heterojunction bipolar transistors[14] and zero-field time of flight techniques in GaAs.[15] Theoretical work focused on device modeling requirements for Si devices identified differences in attractive (majority hole and N_A^- sites) and repulsive (minority electron and N_A^- sites) scattering behavior at lower temperatures.[16,17] Modeling for electron mobility in GaAs also predicted significant differences in temperature dependence compared to majority carrier mobility,[18] but was unable to fully explain the experimental results.[14,15] This emphasizes the importance of direct measurement of the minority carrier mobility, since estimates based on majority carrier mobility trends are not reliable, as functions of either doping or temperature.

In summary, we have directly measured minority carrier diffusion length and minority carrier lifetime as a function of temperature in $\sim 10^{17}\,cm^{-3}$ doped and nominally undoped ($\sim 10^{15}$–$10^{16}\,cm^{-3}$) p-type GaInP via transport imaging and TRPL over a temperature range from 300 K to 5 K. Minority electron mobilities were then determined as a function of temperature, indicating dominant scattering contributions from polar optical phonons and alloying. Minority carrier scattering from ionized dopants is less significant at lower temperatures than majority carrier scattering, resulting in a monotonically increasing minority carrier mobility with decreasing temperature for the doping levels studied here. The data are determined from direct optical measurements, as opposed to the fitting of device results that can involve multiple fitting parameters, and provide direct access to the minority carrier mobility. These results should be useful in device modeling and optimization, particularly for multi-junction solar cells and other optoelectronic devices.

Extension to measurement of minority carrier diffusion length at the higher temperatures of interest to solar concentrator applications would be possible with the use of a heating stage in the transport imaging system.

This work was supported at the Naval Postgraduate School in part by National Science Foundation Grant No. DMR-0804527 and in part by the NPS Energy Academic Group with funding from the Navy Energy Coordination Office. T.C. acknowledges support from the Department of Energy, Office of Science Graduate Fellowship Program (DOE SCGF), made possible in part by the American Recovery and Reinvestment Act of 2009, administered by ORISE-ORAU under Control No. DE-AC05-06OR23100. TRPL work at NREL was supported by the Department of Energy Office of Science, Basic Energy Sciences under DE-AC36-08GO28308.

[1]M. A. Green, K. Emery, Y. Hishikawa, W. Warta, and E. D. Dunlop, Prog. Photovoltaics **21**, 1 (2013); See http://www.nrel.gov/ncpv/images/efficiency_chart.jpg for information regarding maximum solar cell efficiencies over time.
[2]S. Kurtz and J. Geisz, Opt. Express **18**, A73 (2010).
[3]D. R. Luber, F. M. Bradley, N. M. Haegel, M. C. Talmadge, M. P. Coleman, and T. D. Boone, Appl. Phys. Lett. **88**, 163509 (2006).
[4]N. M. Haegel, T. J. Mills, M. Talmadge, C. Scandrett, C. Frenzen, H. J. Yoon, C. Fetzer, and R. King, J. Appl. Phys. **105**, 023711 (2009).
[5]N. M. Haegel, S. E. Williams, C. L. Frenzen, and C. Scandrett, Semicond. Sci. Technol. **25**, 055017 (2010).
[6]H. S. Bennett, J. Appl. Phys. **80**, 3844 (1996).
[7]H. Ehnenreich, J. Phys. Chem. Solids **8**, 130 (1959).
[8]M. A. Littlejohn, J. R. Hauser, T. H. Glisson, D. K. Ferry, and J. W. Harrison, Solid-State Electron. **21**, 107 (1978).
[9]C. Besikci and M. Razeghi, IEEE Trans. Electron Devices **41**, 1066 (1994).
[10]B. Zhang, S. Lan, L.-Q. Li, W.-J. Xu, C.-Q. Yan, and H.-D. Liu, Solid State Commun. **92**, 419 (1994).
[11]I. T. Yoon, S. J. Oh, and H. L. Park, J. Appl. Phys. **83**, 1527 (1998).
[12]S. E. Swirhun, D. E. Kane, and R. M. Swanson, IEEE Trans. Electron Devices **ED-34**, 2385 (1987).
[13]C. H. Wang, K. Misiakos, and A. Neugroschel, Appl. Phys. Lett. **57**, 159 (1990).
[14]K. Beyzavi, K. Lee, D. M. Kim, M. I. Nathan, K. Wrenner, and S. L. Wright, Appl. Phys. Lett. **58**, 1268 (1991).
[15]M. Lovejoy, M. R. Melloch, and M. S. Lundstrom, Appl. Phys. Lett. **67**, 1101 (1995).
[16]D. B. M. Klaassen, Solid-State Electron. **35**, 953 (1992).
[17]D. B. M. Klaassen, Solid-State Electron. **35**, 961 (1992).
[18]W. Walukiewicz, J. Lagowski, L. Jastrezebski, and H. C. Gatos, J. Appl. Phys. **50**, 5040 (1979).